

Light-cone-quantized QCD in 1 + 1 dimensions

Kent Hornbostel

Newman Laboratory of Nuclear Studies, Cornell University, Ithaca, New York 14853

Stanley J. Brodsky

Stanford Linear Accelerator Center, Stanford University, Stanford, California 94309

Hans-Christian Pauli

Max Plank Institute for Nuclear Physics, D-6900 Heidelberg 1, Germany

(Received 5 February 1990)

The QCD light-cone Hamiltonian in one space and one time dimension is diagonalized in a discrete momentum-space basis. The hadronic spectrum and wave functions for various coupling constants, numbers of color, and baryon number are computed.

I. INTRODUCTION

Quantum chromodynamics (QCD) potentially describes all of hadronic and nuclear physics in terms of quarks and gluons as fundamental degrees of freedom. Many features of the theory are consistent with experiment, especially at large momentum transfer where asymptotic freedom allows perturbative predictions. However, confrontation with the most significant and intrinsically nonperturbative aspects of the theory, its predictions for the spectrum and wave functions of hadrons, as well as the mechanisms for confinement and jet hadronization still must wait for theoretical solutions.

In this paper, the application to QCD in 1+1 dimensions of a general nonperturbative approach to field theory [discretized light-cone quantization (DLCQ)] developed in Ref. 1 is presented,^{2,3} and the prospects for 3+1 dimensions are briefly discussed.

SU(N) gauge theories restricted to one spatial dimension and time were introduced by 't Hooft⁴ and have been studied extensively, both analytically and numerically,⁵ predominantly for the case when N is large. There are some special properties of these theories peculiar to 1+1 dimensions which should be mentioned for the sake of orientation. Because there are no transverse directions, the gluons are not dynamical, and (in the $A^+=0$ gauge) their presence is felt only by the constraint equation they leave behind. Likewise the quarks carry no spin. The fermion field may be represented as a two-component spinor, and chirality for massless fermions identifies only the direction of motion. The coupling constant g carries the dimension of mass, and for one quark flavor of mass m , the relevant parameter is g/m (Ref. 6). After the subtraction of infinite constants, the theory is finite. Finally, the restriction to one spatial dimension produces confinement automatically, even for (1+1)-dimensional (QED)₁₊₁. The electric field is unable to spread out and the energy of a nonsinglet state diverges as the length of the system.

In spite of these idiosyncrasies, these models possess certain qualities to commend their study, not the least be-

ing tractability. There are only so many opportunities in a lifetime to solve, albeit numerically, a confining field theory with arbitrary coupling from first principles. With solutions in hand, conceptual questions, points of principle, or approximation schemes which do not depend on the dimensionality of the model may be addressed.⁷

Also, these models provide a test bed for approximation schemes and numerical techniques which may prove useful for realistic problems and a check on approximations, such as the large- N expansion, already in use. Finally, if these models cannot be solved, there is no hope for solving QCD in 3+1 dimensions.

II. LIGHT-CONE QUANTIZATION

Quantization on the light cone is formally similar to standard canonical equal-time quantization, but with a few technical differences which nevertheless make life much easier. Given a (Lorentz-invariant) Lagrangian $\mathcal{L}(x^\mu)$, a new variable $x^+ \equiv x^0 + x^3$ is defined to play the role of time, along with new spatial variables (in four dimensions), $x^- \equiv x^0 - x^3$ and $x_\perp \equiv (x^1, x^2)$. Independent degrees of freedom are identified by the equations of motion. These are initialized to satisfy canonical commutation relations at $x^+ \equiv 0$, and the creation and annihilation operators from their momentum-space expansion define the Fock space. The momenta conjugate to x^- and x_\perp , P^+ and P_\perp , respectively, are diagonal in this space and conserved by interactions. P^- acts as a Hamiltonian; in general it is complicated, dependent on the coupling constant, and it generates evolution in x^+ . Diagonalizing it is equivalent to solving the equations of motion.

The mass-shell condition, $p^2 = m^2$, for individual quanta implies that $p^- = (m^2 + p_\perp^2)/p^+$, so that positive (light-cone) energy quanta must also carry positive p^+ . This seemingly innocent detail is crucial; the positivity of p^+ combined with its conservation is responsible in large part for the simplicity of this approach. First, x^+ -ordered perturbation theory becomes computationally vi-

able because a large class of diagrams which appear in the time-ordered analog vanish.⁸ These include any diagram containing a vertex in which quanta are created out of the vacuum. Since all p^+ are positive, at such a vertex the total momentum cannot be conserved.

More importantly for the work described here, but by essentially the same reasoning, the perturbative vacuum is an eigenstate of the full, interacting Hamiltonian, with eigenvalue zero. Quanta cannot be produced from the vacuum and still conserve p^+ (Ref. 9). One very desirable feature of this remarkable fact is that not only is the ground state trivial, but also that all the quanta occurring in higher states are associated with meson and baryon wave functions rather than disconnected pieces of the vacuum.

Finally, light-cone quantization simplifies the numerical work, especially in 1+1 dimensions. The analysis is essentially frame independent; no absolute Lorentz frame is specified.¹ The system is quantized in a box of length $2L$ in the x^- direction with appropriate boundary conditions so that momenta are discrete and Fock-space states denumerable. For the fixed total momentum P^+ , the relevant dimensionless momentum will be $K=(L/2\pi)P^+$. To see how K restricts the space of states, consider $K=3$, which must be partitioned among the quanta in each state. The only three possibilities are (3), (2,1), and (1,1,1). We can contrast this with equal-time Fock states of definite P^+ ; for equivalent numerical momentum, partitions will include not only those enumerated above, but also (4,-1), (104,-101), (5,5,3,1,-1,-10), and so on. To keep the number of states finite, an additional cutoff in momentum must be introduced, whereas this is not necessary in the light-cone case.

Not only does a fixed K act implicitly as a momentum cutoff, it also severely limits both the total number of states of definite momentum and the number of quanta in each individual state, as the example above demonstrates. K serves one more role. The continuum limit $L \rightarrow \infty$ is equivalent to $K \rightarrow \infty$ as the physical momentum P^+ remains fixed. The size of K determines the physical size of the system, or equivalently, the fineness of the momentum-space grid.

III. $SU(N)_{1+1}$ ON THE LIGHT-CONE

An $SU(N)$ gauge theory is defined by the Lagrangian

$$\mathcal{L} = -\frac{1}{4}F^{\mu\nu a}F_{\mu\nu}^a + \bar{\psi}(i\not{D} - m)\psi. \quad (1)$$

$F_{\mu\nu}^a$ is the field-strength tensor $F_{\mu\nu}^a = \partial_\mu A_\nu^a - \partial_\nu A_\mu^a - gf^{abc}A_\mu^b A_\nu^c$ and the covariant derivative is defined as $i\not{D}_\mu = i\partial_\mu - gA_\mu^a T^a$. In two dimensions, the fermion field $\psi = (\psi_L(x)_c, \psi_R(x)_c)$ (in a representation in which γ^5 is diagonal) is a two-component spinor in the fundamental representation. The subscripts L and R identify chirality, which for massless fermions specifies only direction of motion.

A useful gauge choice is $A^+ = 0$. In this gauge there are neither ghosts nor negatively normed gauge bosons, so the Fock-space quanta, and therefore the wave-function constituents are physical and positively normed.

Also, in 1+1 dimensions, this gauge choice is Lorentz, but not parity, invariant. The equations of motion are then

$$i\partial_- \psi_L = \frac{1}{2}m\psi_R, \quad (2)$$

$$-\partial_-^2 A^- = g\psi_R^\dagger T^a \psi_L \equiv \frac{1}{2}gj^{+a}, \quad (3)$$

$$i\partial_+ \psi_R = \frac{1}{2}gA^- T^a \psi_L + \frac{1}{2}m\psi_L, \quad (4)$$

$$\partial_+ \partial_- A^- = g\psi_L^\dagger T^a \psi_L - \frac{1}{2}gf^{abc}\partial_- A^{-b} A^{-c} \equiv \frac{1}{2}gj^{-a}. \quad (5)$$

Only Eqs. (4) and (5) are dynamical; these will be generated by the Hamiltonian P^- . Equations (2) and (3) are constraints, as they involve only derivatives in x^- . At each time x^+ , both ψ_L and A^- may be solved for in terms of ψ_R by inverting these derivatives with appropriate Green's functions.

The field ψ_R is evidently the only independent degree of freedom and as such is the only field quantized.¹¹

The standard canonical anticommutator

$$\{\psi_R(x)_c, \psi_R^\dagger(y)^{c'}\}_{x^+=y^+} = \delta_{c_1}^{c_2} \delta(x^- - y^-) \quad (6)$$

may be implemented at $x^+ = 0$ by expanding in terms of creation and annihilation operators:

$$\psi_R(x^-)_c = \frac{1}{\sqrt{2L}} \sum_{n=1/2, 3/2, \dots}^{\infty} (b_{n,c} e^{-i(n\pi/L)x^-} + d_{n,c}^\dagger e^{i(n\pi/L)x^-}). \quad (7)$$

The operators which generate translations in x^μ are derived from the energy-momentum tensor:

$$P^\mu = \frac{1}{2} \int dx^- \Theta^{+\mu}. \quad (8)$$

The momentum conjugate to $x^-, P^+ = \sum_n k_n^+ (b_n^\dagger c b_{n,c} + d_{n,c}^\dagger d_n^c)$, is diagonal while P^- , which generates evolution in x^+ , is in general complicated and dependent on the coupling g . Diagonalizing P^- is equivalent to solving the equations of motion. In this discussion, the role of boundary terms is explicitly ignored. A more complete discussion is given in Ref. 12.

The full Hamiltonian P^- in the space of color singlets may be divided into $P^- = m^2 H_0 + g^2 H_I$. The free Hamiltonian, $m^2 H_0$, assigns an energy m^2/k^+ to each quark, while the interacting piece is given by

$$g^2 H_I = -\frac{1}{4}g^2 \int dx^- dy^- |x^- - y^-| j^{+a}(x^-) j^{+a}(y^-), \quad (9)$$

where the current is the normal-ordered product $j^{+a} = 2:\psi_R^\dagger T^a \psi_R:$. The potential $|x^- - y^-|$ is the result of inverting the constraint equation (3) for A^- .

Finally, the interaction may be divided into a part H_I which is entirely normal ordered [Fig. 1(b)] and a remaining diagonal part H_I^{diag} [Fig. 1(a)] which contains a quark mass renormalization. The linear potential in position space becomes the instantaneous gluon propagator $(1/p^+)^2$ in momentum space. Interactions in which zero p^+ are exchanged couple to the total charge operator Q^a ,

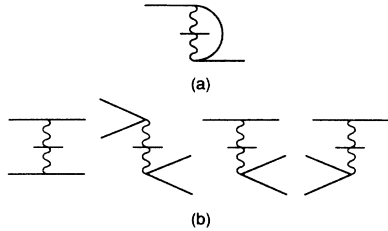


FIG. 1. Interaction vertices.

and so are discarded in the color-singlet sector. Typical four-quark interactions in H_I have the form

$$\frac{L}{2\pi} \frac{g^2}{\pi} \frac{1}{2} \left[\delta_{c_4}^{c_2} \delta_{c_1}^{c_3} - \frac{1}{N} \delta_{c_4}^{c_3} \delta_{c_1}^{c_2} \right] \times \sum_{n_i=1/2, 3/2, \dots} \frac{\delta_{n_1+n_2, n_3+n_4}}{(n_1+n_3)^2} b_{n_4}^{\dagger c_4} b_{n_3, c_3}^{\dagger} d_{n_2, c_2}^{\dagger} d_{n_1}^{c_1}. \quad (10)$$

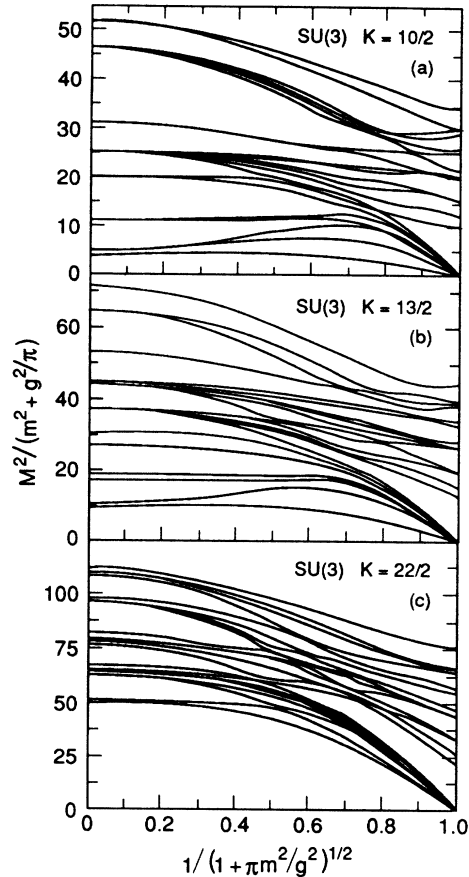
This quantization procedure follows closely that of the Schwinger model discussed in Ref. 13, and so is only surveyed here. For a more complete discussion including the complete Hamiltonian, see Ref. 12.

IV. THE PROGRAM

In order to evaluate and diagonalize P^- numerically, the system is quantized in a box in x^- of length $2L$ and boundary conditions are selected. Consequently, the momenta are discrete and denumerable. In order to expand ψ_R in a complete set of plane-wave solutions of the free equations of motion, antiperiodic boundary conditions are employed. Periodic conditions are not convenient since the term with $k^+ = 0$, necessary for completeness, is not a solution of the free equation $k^+ k^- = m^2$ except when m is zero.¹⁴ The field ψ_R expanded in operators with discrete momenta as in Eq. (7) is then inserted in Eq. (8) to produce the discretized Hamiltonian P^- .

The computer program is set up to run for arbitrary number of colors N , baryon number B , and numerical momentum $K = (L/2\pi)P^+$ (Ref. 15). Given these, it constructs the Fock space by generating all possible distributions of K among quarks in color singlets. In general, this construction is overcomplete. The program then evaluates and diagonalizes the inner-product matrix $\langle i|j \rangle$, identifying redundant states by zero eigenvalues and removing them. Those states remaining are orthonormal and complete.

The Hamiltonian matrix $\langle i|H|j \rangle$ is evaluated in this basis, with the color contractions performed diagrammatically. Because the light-cone Hamiltonian breaks up simply into H_0 multiplied by m^2 and H_I by g^2 , the corresponding matrices are stored separately. Altering g (or m) involves only multiplying these matrices by the new parameter prior to diagonalization, with almost no additional cost in time.¹⁶ Setting g/m , combining H_0 and H_I , and diagonalizing produces the full spectrum, Fig. 2, subject to the limitations imposed by discretization. In-

FIG. 2. Spectra for $N=3$, baryon number $B=0, 1$, and 2 as a function of g/m ; K fixed.

cluded in the spectra are not only single mesons and baryons and their excited states, but also multiple-hadron scattering states. In each case a large number of massless mesons and baryons appear in the strong-coupling (small-mass) limit. The spectrum obtained is the full hadronic spectrum of QCD in one space and one time dimension, consistent with the resolution parameter K .

V. WAVE FUNCTIONS

Diagonalization gives not only eigenvalues but also their eigenvectors; i.e., the light-cone hadronic wave functions. Because the perturbative vacuum is also the fully interacting vacuum, all quanta in the wave functions are associated with mesons and baryons, making them simple to interpret and straightforward to employ in calculations.¹⁷ Expressed in terms of the light-cone momentum fraction $x \equiv k^+/P_{\text{total}}^+$, they are invariant under longitudinal Lorentz boosts, and so, in 1+1 dimensions are Lorentz invariant. Parity is still conserved but more complicated to implement, as it is not respected by the quantization scheme. The parity of nondegenerate states may be identified by tracing the state from weak coupling, where parity is simple, or by examining matrix elements of appropriate odd or even operators.¹⁸ For the special case of $q\bar{q}$ wave functions, odd (even) parity corre-

sponds to evenness (oddness) under interchange of the constituents' momenta.

Finally, these wave functions are universal; they contain all of the information about the hadrons. Once computed, masses, form factors and inclusive and exclusive scattering amplitudes are reduced to computing a few integrals. For example, in four dimensions, the ratio

$$R(Q^2) = (\sigma_{e^+e^- \rightarrow \text{hadrons}} / \sigma_{e^+e^- \rightarrow \mu^+\mu^-}) \quad (11)$$

is a textbook example of a quantity calculable in QCD when Q^2 is large. The relevant matrix element, $(e^2/Q^2)\bar{v}\gamma_\mu u \langle \text{hadrons} | J_{\text{em}}^\mu | 0 \rangle$ is typically squared and related to vacuum-polarization graphs, which are then computed as an expansion in $\alpha_s(Q^2)$. However, given the appropriate hadronic wave functions, this matrix element could be computed directly at any Q^2 . A feature such as the ρ resonance would then appear as an enhancement in the density of states in the $\pi\pi$ continuum. The experimental resolution $\delta s/s$ can be matched to the resolution $1/K$ of the DLCQ analysis.

The valence wave functions for the lightest $N=3$ meson and baryon are displayed in Fig. 3 by means of their quark structure functions:

$$q(x) = K \langle \phi(K) | b_k^\dagger b_{k,c} | \phi(K) \rangle, \quad (12)$$

where $x = k/K$. In deep-inelastic scattering x can be identified with the Bjorken variable $x_{bj} = Q^2/2p \cdot q$. For weak coupling ($m/g = 1.6$) the quark mass dominates p^+ and so momentum peaks around equal sharing among constituents: $x = 1/2$ and $1/N$ for the meson and baryon, respectively. Stronger coupling tends to broaden the distribution.

In general, in a quantum field theory the wave functions contain higher-Fock components with additional numbers of quarks. Figures 4(a) and 4(b) illustrate the contribution to the quark structure function from the component of the lightest $N=3$ meson and baryon wave function with an additional $q\bar{q}$ pair. Their contribution is suppressed relative to that of the valence wave function by 2 to 4 orders of magnitude. Because P^+ must be distributed among more quanta, the average x is lower. The characteristic bump structure may be understood in terms of $q\bar{q}$ pairs splitting off of the valence quarks, at least for weak coupling.¹⁹ Figure 4(b) also includes the antiquark functions and gives an indication of what may be thought of as the pion content of the baryon. Figure 4(c) presents the (negligible) contribution from the Fock

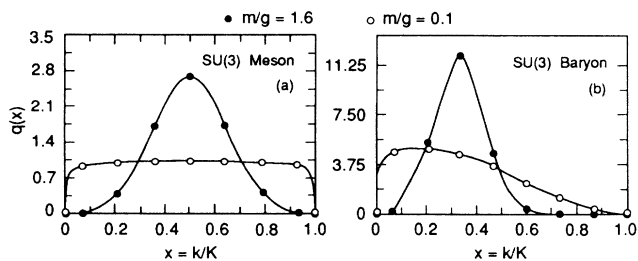


FIG. 3. Valence structure functions for $N=3$ baryon and meson at $m/g=0.1$ and 1.6 .

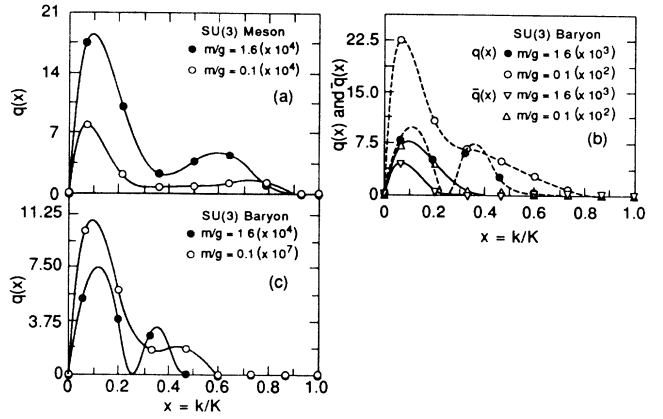


FIG. 4. Higher-Fock contributions to $N=3$ structure functions. (a) Lightest meson. (b) Lightest baryon, including antiquarks. (c) Baryon: contribution from two extra quark pairs. The curves are intended to guide the eye.

state with two extra quark pairs. It is an interesting phenomenological possibility that the true nonvalence Fock-state contribution to hadronic structure functions in $3+1$ dimensions actually has the oscillatory shape of the type obtained here.

Of course, the spectrum consists of many states beyond the lightest. Because the quanta are associated only with the hadron, the wave functions need not be disentangled from the vacuum and are often relatively simple to interpret. In Fig. 5, the first three (weakly coupled) meson wave functions (or, more precisely, structure functions) are clearly the first three radial excitations of a predominantly $q\bar{q}$ state. In fact, in the nonrelativistic limit these become the momentum transforms of Airy functions.²⁰ Figure 5(d) presents the eleventh state, which is located in the continuum. The dominant contribution is from two $q\bar{q}$ pairs peaked at $x = 1/4$, with a mass twice that of the first state; it clearly represents a pair of the lightest mesons. Figure 6 presents a similar picture for the $N=3$

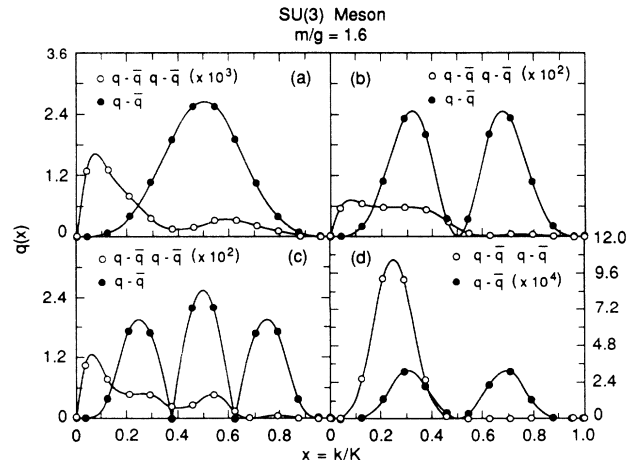


FIG. 5. (a)–(c) First three states in $N=3$ meson spectrum for $m/g=1.6$, $2K=24$. (d) Eleventh state.

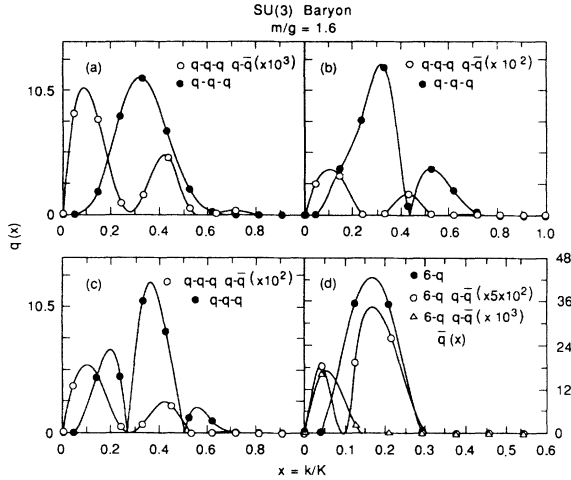


FIG. 6. (a)–(c) First three states in $N=3$ baryon spectrum, $2K=21$. (d) First $B=2$ state.

baryons. The pair of baryons in Fig. 6(d) is selected from the $B=2$ spectrum. For strong coupling, it is more difficult to disentangle states due to the presence of a large number of very light mesons and baryons.

VI. MASSLESS MESONS AND BARYONS IN THE $m/g \rightarrow 0$ LIMIT

The massless hadrons at zero quark mass may be understood by studying the momentum-space transforms of the $SU(N)$ currents (at $x^+=0$)

$$V_k^a = \frac{1}{2} \int_{-L}^L dx^- e^{-i(k\pi/L)x^-} j^+(x^-) \quad (13)$$

which satisfy the Kac-Moody algebra $[V_k^a, V_l^b] = if^{abc} V_{k+l}^c + \frac{1}{2} l \delta^{ab} \delta_{k+l,0}$. The currents j^+ are defined by point splitting along x^- ; for $A^+=0$, the path-ordered exponential included to ensure gauge invariance reduces to one. The algebra may be extended to include the $U(1)$ current $j^+ = (2/N)^{1/2} \psi_R^\dagger \psi_R$. The transformed operator V_k commutes with the other $SU(N)$ elements, and the re-

lated operator $a_k^\dagger \equiv (2/k)^{1/2} \epsilon(k) V_k$ satisfies the free boson commutation relations $[a_k, a_l^\dagger] = \delta_{k,l}$.

The interacting part of the Hamiltonian is greatly simplified when expressed in terms of these operators:

$$P_I^- = \frac{g^2}{16} \int_{-L}^L dx^- dy^- |x^- - y^-| j^+(x^-) j^+(y^-) \quad (14)$$

becomes

$$\frac{L}{2\pi} \frac{g^2}{2\pi} \sum_{k=-\infty}^{\infty} \frac{1}{k^2} V_k^a V_{-k}^a. \quad (15)$$

Because $V_{k=0}^a = Q^a$, the contribution at $k=0$ is proportional to the total charge $Q^a Q^a$ and so may be discarded in the singlet sector.

The V_k are color-singlet bilinear operators in ψ_R , and so may be used to create mesonlike states with momentum $P^+ = 2\pi k/L$. In the limit where m/g is zero, the entire Hamiltonian is given by Eq. (15). Because the V_k commute with the V_k^a which appear in P_I^- ,

$$M^2 V_k |0\rangle = \frac{2\pi k}{L} [P^-, V_k] |0\rangle = 0. \quad (16)$$

Not only is the state created by acting with V_k on the vacuum an exactly massless eigenstate in this limit, but states formed by repeated applications are also exactly massless. Furthermore, acting with V_k on an eigenstate of nonzero mass produces a degenerate state of opposite parity as k approaches zero. These arguments are independent of the value of the numerical momentum K and so give an exact continuum result.

Just as the existence and number of massless states is most simply discussed in terms of the V_k , so also are the wave functions of these states. Applying one V_k to the vacuum

$$V_K |0\rangle = \frac{1}{\sqrt{2N}} \sum_{n=1/2, 3/2, \dots}^{K-(1/2)} b_{K-n}^{\dagger c} d_{n,c}^\dagger |0\rangle \quad (17)$$

yields a continuum wave function of $\phi(x)=1$ (where $n/K \rightarrow x$). Because ϕ is even under the interchange of x and $1-x$, this state is a pseudoscalar. The wave functions of momentum K created by applying V twice are, for any $l < K$,

$$V_{K-l} V_l |0\rangle = \frac{1}{2N} \left[\sum_{n=1/2}^{l-(1/2)} (b_{K-n}^{\dagger c} d_{n,c}^\dagger - b_n^{\dagger c} d_{K-n,c}^\dagger) + \sum_{m=1/2}^{K-l-(1/2)} \sum_{n=1/2}^{l-(1/2)} b_{K-l+m}^{\dagger c_2} d_{m,c_2}^\dagger b_{l-n}^{\dagger c_1} d_{n,c_1}^\dagger \right] |0\rangle. \quad (18)$$

The $q\bar{q}$ piece is odd; therefore this state is a scalar, as a product of pseudoscalars must be. All the massless meson wave functions for a given K may be constructed in this manner; parity will alternate with each additional V .

If the gauge group had been $U(N)$ rather than $SU(N)$ (Ref. 21) an additional term associated with the extra $U(1)$,

$$\frac{L}{2\pi} \frac{g^2}{2\pi} \sum_{k=1}^{\infty} a_k^\dagger a_k, \quad (19)$$

would appear in P^- . The a_k satisfy free bosonic commutation relations, and this additional interaction is therefore the discrete light-cone Hamiltonian for free bosons of mass squared $g^2/2\pi$. These formerly massless states created by the a_k are promoted to the free massive bosons found in the Schwinger model and discussed in Refs. 13 and 22. Though now massive, the wave functions for these states remain unchanged.

Note that while the entire $U(1)$ spectrum may be built up entirely from these noninteracting bosons,¹³ for $U(N)$ or $SU(N)$ they describe only part of the spectrum; these

are the massless mesons for $SU(N)$. In addition there are massive states which include excited $q\bar{q}$ pairs.

Similarly, the composite baryon field

$$B_k \equiv \frac{1}{2} \int_{-L}^L dx^- e^{-i(k\pi/L)x^-} \epsilon_{c_1 \dots c_N} \psi_R^{\dagger c_1}(x^-) \dots \psi_R^{\dagger c_N}(x^-) \quad (20)$$

commutes with the V_k^a , and, in the limit $m/g \rightarrow 0$, with the Hamiltonian P^- . As in the case for mesons, this field creates an identically massless baryon. Repeated applications on the vacuum produce a massless state with arbitrarily desired baryon number. Furthermore, degenerate states with the same baryon number may be created by acting with the massless mesonic operators $V_{k=0}$ in conjunction with the B_k . Again, these results are independent of K and are true in the continuum limit. The (unnormalized) wave function associated with this massless baryon is

$$B_k |0\rangle = \frac{1}{2(2L)^{(N-1)/2}} \sum_{n_i} \delta_{K, \sum n_i} \epsilon_{c_1 \dots c_N} b_{n_1}^{\dagger c_1} \dots b_{n_N}^{\dagger c_N} |0\rangle. \quad (21)$$

Whether this state is a fermion or boson depends on N being odd or even. The quark distribution derived from this wave function for $N=3$ becomes $6(1-x)$ in the continuum limit; this x dependence is clearly evident in Fig. 3. The general expression for the quark distribution for a single baryon in the $m/g \rightarrow 0$ limit is

$$q(x) = N(N-1)(1-x)^{N-2}. \quad (22)$$

For $N=2$, $q(x)=2$, which apart from the normalization, is identical to the meson distribution for all N .

VII. NUMERICAL ACCURACY

A great deal of information about solutions in the continuum limit may be extracted by restricting the Fock space to a single $q\bar{q}$ pair. This is a good approximation to the lightest meson and its radial excitations, but it neglects a large part of the low-lying spectrum when g/m is large.

Restricting the eigenvalue equation

$$M^2 |\phi(P^+)\rangle = P^- P^+ |\phi(P^+)\rangle \quad (23)$$

to the $q\bar{q}$ subspace and taking the limit $K \rightarrow \infty$ yields the integral equation²³

$$\begin{aligned} M^2 \phi(x) = & m^2 \left[\frac{1}{x} + \frac{1}{1-x} \right] \phi(x) \\ & - \frac{g^2}{\pi} \left[\frac{N^2 - \alpha}{2N} \right] P \int_0^1 dy \frac{\phi(y) - \phi(x)}{(y-x)^2} \\ & + \frac{g^2}{\pi} \left[\frac{(1-\alpha)N}{N} \right] \int_0^1 dy \phi(y). \end{aligned} \quad (24)$$

For $SU(N)$, $\alpha=1$, and $\alpha=0$ for $U(N)$. The continuum wave function $\phi(x)$ is defined by

$$\begin{aligned} |\phi(P^+)\rangle = & \int_0^1 \frac{dx}{[4\pi N x(1-x)]^{1/2}} \\ & \times \phi(x) b_{(1-x)P^+}^{\dagger c} d_{xP^+,c}^{\dagger} |0\rangle. \end{aligned} \quad (25)$$

This equation incorporates all of the leading-order dynamics of the large- N approximation.⁴ Because it could be derived from the discretized Hamiltonian in the continuum limit $K \rightarrow \infty$, it demonstrates that this limit is sensible. Also, it shows trivially that, when $m=0$, $\phi(x)=1$ is an eigenfunction with $M^2=0$ for $SU(N)$, $g^2/2\pi$ for $U(N)$. The latter is the well-known Schwinger model boson.

More importantly for this work, it shows the error due to discretization as that of an integral evaluated numerically on a regularly spaced grid, with spacing $\epsilon=1/K$. This is not normally an efficient method, and this case is not even normal. In addition to the typical errors of order ϵ^n , $n \geq 2$, the principal-value-regulated singularity in Eq. (24) induces an error of order ϵ . Also, for small x , $\phi(x) \propto x^a$, with a given implicitly by⁴

$$1 - a\pi \cot(a\pi) = \frac{\pi m^2}{g^2 \left[\frac{N^2 - 1}{2N} \right]}, \quad (26)$$

and ranging from zero (when $m/g=0$) to one ($g/m=0$). This nonanalytic end-point behavior produces additional a -dependent errors. As a result, a physical quantity such as a mass measured at finite K behaves as

$$M(1/K) = M(0) + \frac{c_1}{K} + \frac{c_2}{K^{1+a}} + \frac{c_3}{K^2} + \frac{c_4}{K^{2+a}} + \dots \quad (27)$$

with $M(0)$ the continuum limit. This behavior, as well as Eq. (26), apply as well to baryons and higher-Fock states.¹² Knowing Eq. (27), the convergence may be improved significantly by Richardson extrapolation; that is, by computing M at n different K and fitting to Eq. (27). An estimate of the error in determining $M(0)$ is then given by the n th term. This extrapolation has allowed for meaningful numerical results from the relatively low $K \approx 10$, as well as for error estimates.

The masses of the lowest-lying states are generally of the most interest and are the quantities most likely available for comparison from other methods, especially lattice calculations. The masses of the lowest-lying meson and baryon for N of 2, 3, and 4 at a selected set of couplings are listed in Table I and displayed in Fig. 7.

In all cases, that is at every m/g and K , the lightest $N=2$ meson and baryon have identical masses, and $M_{\text{mes}}/M_{\text{bar}}=1$ for $N=2$ is an exact result. The results quoted in Table I are extrapolations to continuum results by matching to a series in $1/K$ for $2K$ in the range of roughly 16–24, and the numbers in parentheses give the magnitude of the last term in the series fit. For $m/g \gtrsim 0.2$, these are reasonable estimates of the actual error. Beyond this, the largest K employed is likely not large enough for these to be more than a rough guide. However, when $m/g=0$ identically, the lightest state for any N or B is exactly zero, independently of K .

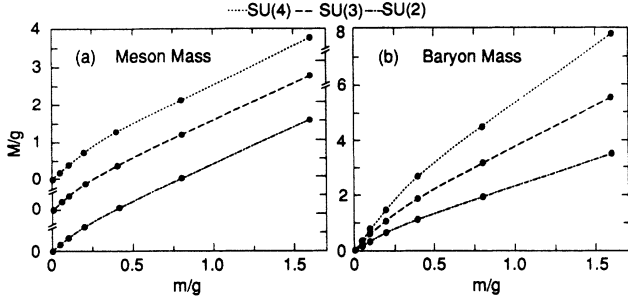


FIG. 7. Extrapolated masses for $N=2, 3,$ and 4 meson and baryon.

Finally, these data may be compared with previous calculations. Figure 8(b) demonstrates the rapid meson mass approach to the large- N limit from Ref. 4 as N increases from two to four. In Fig. 8(a), points from the Hamiltonian lattice calculation of Hamer for $N=2$ agree well with the light-cone results.⁵ This is gratifying in that, while both techniques possess peculiarities, they are peculiar in different ways. Also, the ratio of lightest meson to baryon masses in the strong-coupling limit for $N=2, 3,$ and 4 are consistent, to within the roughly 10% error, with the ratio $2 \sin[\pi/2(2N-1)]$ derived by bosonization.²⁴

VIII. LARGE- N APPROXIMATION

Most previous work on this model employed the large- N approximation to leading order. By obtaining numerical solutions at finite N , the validity of this approximation for interesting values of N such as three can be tested. From Figs. 7 and 8, for weak coupling (large quark mass) it is quite good. The meson mass is already well approximated for $N=2$, and, as expected, the baryon masses increase proportionally with N . The low-lying states are indeed $q\bar{q}$ excitations; higher-Fock contributions are negligible. For strong coupling (small mass), the approximation is not as reliable; the effective expansion parameter g^2N/m^2 is no longer small.²⁵ Light baryons exist for all finite N and so may not be neglected. The low-lying meson spectrum is dominated by states with arbitrary numbers of quarks rather than $q\bar{q}$ excitations. Finally, for $U(N)$, the meson mass (as $m/g \rightarrow 0$) of $g^2/2\pi$ is neglected in the large- N limit.

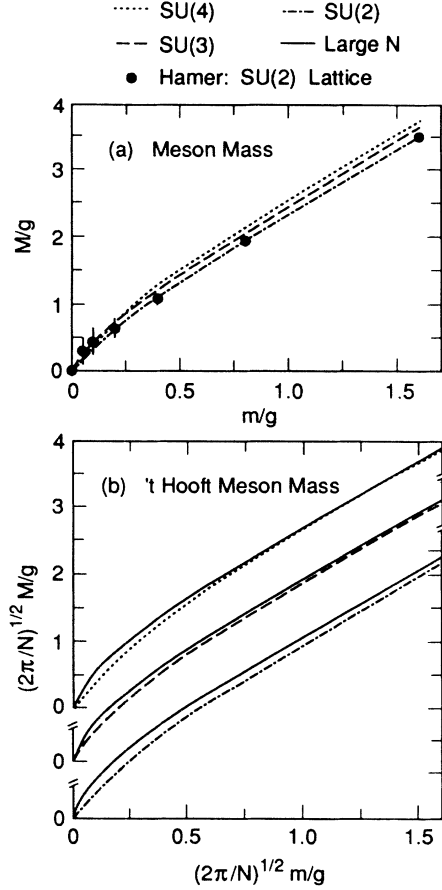


FIG. 8. Comparison of $N=2, 3,$ and 4 meson masses with large- N and lattice calculations.

IX. PROSPECTS IN FOUR DIMENSIONS

In three-plus-one-dimensions, the application of DLCQ to QCD becomes much more challenging, as introducing transverse directions greatly increases the degrees of freedom. Quarks with spin and physical, transversely polarized gluons must be included. Both carry transverse momentum, which may be discretized on a Cartesian grid, $p_{\perp}^i = (2\pi/L_{\perp})n_{\perp}^i$. The n_{\perp}^i can be negative, and must be restricted by a cutoff. However, in principle, diagonalizing the light-cone Hamiltonian will yield not only the spectrum of QCD, but also the light-cone Fock-state

TABLE I. N dependence of meson and baryon mass.

m/g	$N=2$	M_{mes}/g $N=3$	$N=4$	$N=3$	M_{bar}/g $N=4$
1.6	4.314(4)	4.618(6)	4.845(2)	10.71(2)	21.2(3)
0.8	3.913(4)	4.40(5)	4.743(2)	10.4(1)	20.9(5)
0.4	2.61(5)	3.1(5)	3.4(2)	7.3(6)	15(1)
0.2	1.17(7)	1.5(5)	1.4(1)	3.1(2)	6.0(8)
0.1	0.38(5)	0.5(2)	0.43(5)	1.1(3)	1.9(3)
0.05	0.10(1)	0.2(2)	0.12(1)	0.31(9)	0.42(6)
0	0	0	0	0	0

wave functions needed to compute structure functions for inclusive reactions, distribution amplitudes for exclusive reactions, and the hadronic matrix elements needed for weak-interaction phenomenology.

In contrast with 1+1 dimensions, QCD₃₊₁ requires a nontrivial renormalization. A cutoff may be implemented directly on the space of states by restricting it to those whose invariant mass satisfies¹⁷

$$M^2 = \sum \frac{k_{\perp}^2 + m^2}{x} < \Lambda^2. \quad (28)$$

The cutoff Λ must be sufficiently larger than the scale of interest, with physics beyond it absorbed into the couplings and masses. One can also restrict the kinetic part of the mass of the intermediate state in order to focus the physics on the nonrelativistic binding regime.²⁶ We are also exploring the use of broken supersymmetry as a gauge-invariant ultraviolet regulator of non-Abelian gauge theories, as an alternative to Pauli-Villars methods.²⁷ Gauge invariance of the light-cone Hamiltonian approach may be checked by showing, for example, that in the continuum and large- Λ limits matrix elements such as $q_{\mu} \langle 0 | j^{\mu} | q \rangle$ vanish, and, for QED, that the photon remains massless.

A crude estimate of the difficulty of the (3+1)-dimensional problem may be made by selecting minimum appropriate values for Λ of 1 GeV and 1 fm for $(L_{\perp}/2\pi)$. These correspond, by Eq. (28), to $x \sim 1/K \sim 1/25$ and $n_{\perp} \sim 5$. This allows some hope that systems with a longitudinal momentum K comparable to that used in 1+1 dimensions combined with the first several transverse modes may begin to provide a recognizable picture of hadronic physics. Presently, programs for diagonalizing the light-cone Hamiltonian for QED₃₊₁ (Refs. 26 and 28) and QCD₃₊₁ (Ref. 26) are under investigation. In the cases where one is interested in only determining the lowest levels, a variational method can be used. An initial study of the lowest eigensolutions of positronium at large α has recently been carried out utilizing this method.²⁸

ACKNOWLEDGMENTS

This work was supported in part by the Department of Energy, Contract No. DE-AC03-76SF00515, and the National Science Foundation. We thank A. Tang, M. Kaluza, and T. Eller for helpful conversations. S.J.B. wishes to acknowledge the support of the Alexander von Humboldt Foundation and the hospitality of the Max-Planck-Institute for Nuclear Physics, Heidelberg.

¹H. C. Pauli, and S. J. Brodsky, Phys. Rev. D **32**, 1993 (1985); **32**, 2001 (1985).

²An initial report on this work was given by K. Hornbostel, S. J. Brodsky, and H. C. Pauli, in *Relativistic Nuclear Many-Body Physics*, proceedings of the Workshop, Columbus, Ohio, 1988, edited by B. C. Clark, R. J. Perry, and J. P. Vary (World Scientific, Singapore, 1989).

³Some of these results have also been obtained by M. Burkhardt, Nucl. Phys. **A504**, 762 (1989). Burkhardt also derives and verifies a new type of virial theorem for bound states in 1+1 dimensions. A detailed discussion of the deuteron two-baryon solutions of QCD₁₊₁ is also given in this reference.

⁴G. 't Hooft, Nucl. Phys. **B75**, 461 (1974).

⁵For a survey up to 1981 along with SU(2) lattice results, see C. J. Hamer, Nucl. Phys. **B195**, 503 (1982).

⁶A. J. Hanson, R. D. Peccei, and M. K. Prasad, Nucl. Phys. **B121**, 477 (1977).

⁷See, for example, J. Briere and H. Kroger, Phys. Rev. Lett. **63**, 848 (1989).

⁸S. Weinberg, Phys. Rev. **150**, 1313 (1966).

⁹This is certainly not the last word on this subject. For instance, this is not strictly true if there are quanta for which p^+ is zero; see, for example, A. Harindranath and J. Vary, Phys. Rev. D **37**, 3010 (1988) and F. Lenz, University of Erlangen report, 1989 (unpublished). There are other subtleties connected with the contrasting vacuum structure on the light-cone and equal-time theories which will be addressed in future work.

¹⁰Pauli and Brodsky, (Ref. 1).

¹¹For an introduction to light-cone quantization, see T.-M. Yan, Phys. Rev. D **7**, 1780 (1972), and references therein. For a discussion of the boundary-value problem and gauge invariance of massless 1+1 light-cone gauge theories, see G. McCartor, Z. Phys. C **41**, 271 (1988).

¹²K. Hornbostel, Ph.D. thesis, SLAC Report No. 333, 1988.

¹³T. Eller, H. C. Pauli, and S. J. Brodsky, Phys. Rev. D **35**, 1493 (1987).

¹⁴We thank A. Tang and G. McCartor for discussions on this point.

¹⁵Multiple flavors can also be incorporated; the results will be reported in a subsequent publication.

¹⁶Typical cases presented here required a total of one to three minutes of CPU on an IBM 3081.

¹⁷For a general review of wave functions in QCD, and their relation to observables such as structure functions and form factors, see G. P. Lepage, S. J. Brodsky, T. Huang, and P. B. Mackenzie, in *Particles and Fields-2*, proceedings of the Banff Summer Institute, Banff, Canada, 1981, edited by A. Z. Capri and A. N. Kamal (Plenum, New York, 1983); G. P. Lepage, and S. J. Brodsky, Phys. Rev. D **22**, 2157 (1980).

¹⁸C. G. Callan, N. Coote, and D. J. Gross, Phys. Rev. D **13**, 1649 (1976).

¹⁹R. Blankenbecler (private communication).

²⁰C. J. Hamer, Nucl. Phys. **B121**, 159 (1977); **B132**, 542 (1978).

²¹This is the group considered by 't Hooft (Ref. 4). The two are equivalent in the large- N limit. In general the extra U(1) introduced need not be associated with the same coupling constant as SU(N), but this is sufficient for this discussion.

²²H. Bergknoff, Nucl. Phys. **B122**, 215 (1977).

²³T. Eller, Ph.D. thesis, Max Planck Institute for Nuclear Physics, Heidelberg, 1987.

²⁴G. D. Date, Y. Frishman, and J. Sonnenschein, Nucl. Phys. **B283**, 365 (1987); J. Sonnenschein (private communication).

²⁵A. Patrascioiu, Phys. Rev. D **15**, 3592 (1977); M. H. Partovi, *ibid.* **22**, 2032 (1980).

²⁶H. C. Pauli *et al.* (in progress).

²⁷S. J. Brodsky, M. Kaluza, and H. C. Pauli (in progress).

²⁸A. Tang, Ph.D. thesis, 1990.